

## SEISMIC RESPONSE OF NTT KOBE EKIMAE BUILDING WITH CONSIDERATION OF NONLINEAR SOIL-STRUCTURE INTERACTION DURING THE 1995 HYOGO-KEN-NANBU EARTHQUAKE

Taku INABA<sup>1</sup>, Hiroshi DOHI<sup>2</sup>, Kenji OKUTA<sup>3</sup>, Taku SATO<sup>4</sup> And Hisanobu AKAGI<sup>5</sup>

### SUMMARY

The seismic response characteristics of NTT Kobe Ekimae Building during the 1995 Hyogo-ken Nanbu Earthquake were estimated by means of a nonlinear soil-structure interaction analysis using the two-dimensional FEM model. The validity of this model was confirmed through the simulation of observed seismic waves on the 8th floor and the 3rd basement of the building. The relation between the ground motion and the damage of the building was quantitatively estimated by the maximum relative story displacement of the building. As the result, the site nonlinearity has a large influence on the amplification characteristics of the surface soil, and the local nonlinearity caused by rocking of building has a large influence on the seismic response characteristics of the building.

### INTRODUCTION

The Hyogo-ken Nanbu Earthquake of 17th January 1995 brought about an enormous damage to structures in the Hanshin and Awaji areas. After the earthquake, the characteristics of the ground motion and the damage to the structures have been investigated from the viewpoint of seismology, earthquake engineering and structural engineering. It is pointed out the importance of investigating the relationship between the ground motion and the damage to buildings.

In order to evaluate quantitatively relationship between the ground motion and the damage to the buildings and to predict accurately a seismic motion entering to the building, it is necessary to make sure the effect of the soil-structure interaction on the nonlinear behavior of surface soil during the strong motion (Dohi et al. 1998).

The strong seismic motions were observed at the 8th floor and the 3rd basement of the NTT Kobe Ekimae Building during the 1995 Hyogo-ken Nanbu Earthquake. In this study, the seismic response characteristics of NTT Kobe Ekimae building was discussed by means of a nonlinear soil-structure interaction analysis using the two-dimensional FEM model. The nonlinear behavior of the soil was evaluated by means of the total stress analysis using the nonlinear step-by-step integration method.

### THE NTT KOBE EKIMAE BUILDING AND SOIL SEDIMENT STRUCTURE

The NTT Kobe Ekimae Building (built in 1972, lat. 34°41'10" N. and long. 135°12' 24" E.) is situated in the area which was designated as 6th degree seismic intensity of Japan Meteorological Agency at the 1995 Hyogo-ken Nanbu Earthquake. The distance from epicenter to the building is about 17km. Figure 1 shows the location of the site and the causative fault. Figure 2 shows the site plan, a plan of the 3rd basement, and a section view of this building. Figure 3 shows the soil profile near the building. The building of a SRC structure has eight stories

<sup>1</sup> Research and Development Department, NTT POWER AND BUILDING FACILITIES INC., Tokyo, Japan, E-mail: inaba@rd.ntt-f.co.jp

<sup>2</sup> Research and Development Department, NTT POWER AND BUILDING FACILITIES INC., Tokyo, Japan, E-mail: inaba@rd.ntt-f.co.jp

<sup>3</sup> Research and Development Department, NTT POWER AND BUILDING FACILITIES INC., Tokyo, Japan, E-mail: inaba@rd.ntt-f.co.jp

<sup>4</sup> Research and Development Department, NTT POWER AND BUILDING FACILITIES INC., Tokyo, Japan, E-mail: inaba@rd.ntt-f.co.jp

<sup>5</sup> Building Engineering Department, NTT BUILDING TECHNOLOGY INSTITUTE, Tokyo, Japan, E-mail: akagi@ntt-bti.co.jp

above the ground and three stories under the ground. Its foundation is a direct foundation on the bearing ground at GL-16m which is composed of sand and gravel layer. The geological data of soil sediment from GL to GL-65m is shown in Table 1. The P-wave and S-wave velocities of the soil sediment are investigated by PS logging. The damage caused by the Hyogo-ken Nanbu Earthquake to this building was relatively slight. The shear ruptures occurred on some of the anti-seismic walls with an opening from the 2nd to 5th story. No more than 1mm wide cracks were observed on the other structural members of the building.

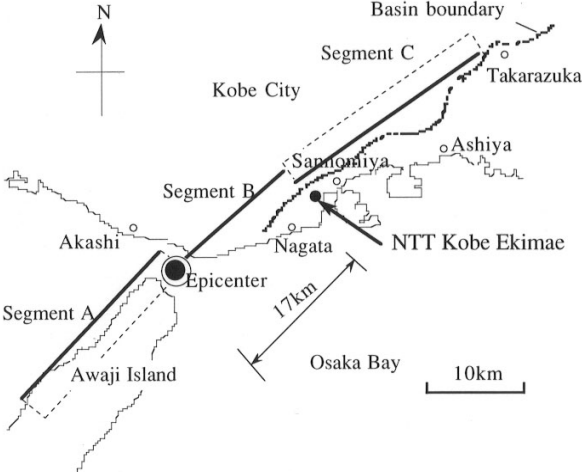


Figure 1: Location of site and causative fault of Hyogo-ken Nanbu Earthquake

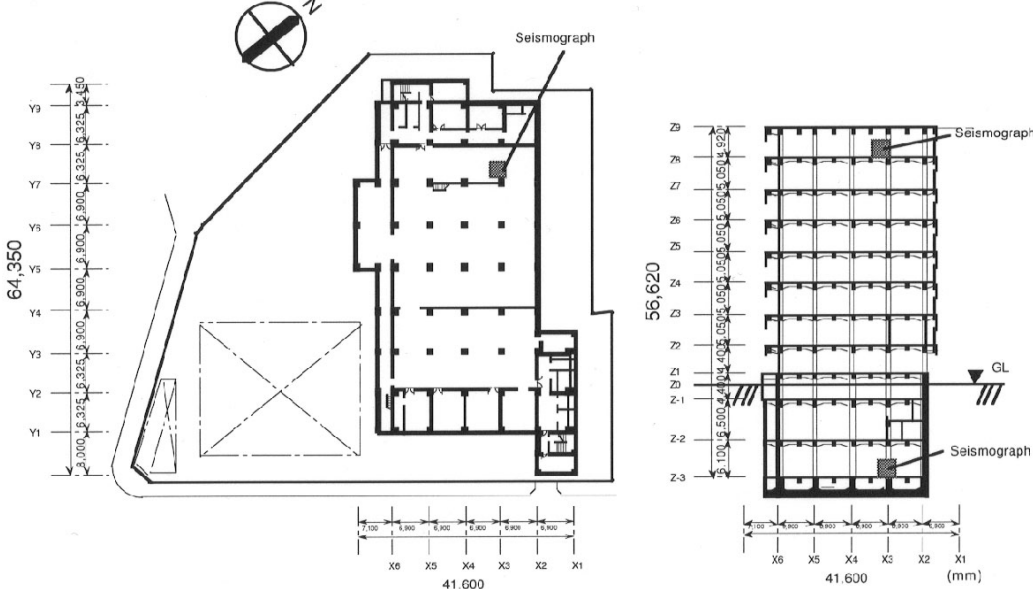


Figure 2: Plan and section view of NTT Kobe Ekimae Building and location of seismograph (in mm)

Table 1: Geological data of soil sediment at the NTT Kobe Ekimae Building

Depth (m)	Soil	Density (g/cm <sup>3</sup> )	Vp (m/s)	Vs (m/s)	Poisson ratio	Damping (%)
GL0-2.0	cobble stone	1.6	410	90	0.475	2.0
2.0-5.0	sand	1.8	1500	130	0.496	2.0
5.0-10.0	sand with gravel	1.9	1500	190	0.492	2.0
10.0-20.0	sandy	1.9	1720	250	0.489	2.0
20.0-38.0	sandy	2.0	1820	410	0.473	2.0
38.0-46.0	clay	2.0	1820	410	0.473	2.0
46.0-52.0	sand with gravel	2.0	1820	410	0.473	2.0
52.0-54.0	sand with gravel	1.9	1620	360	0.474	2.0
54.0-65.0	clay	1.9	1620	360	0.474	2.0

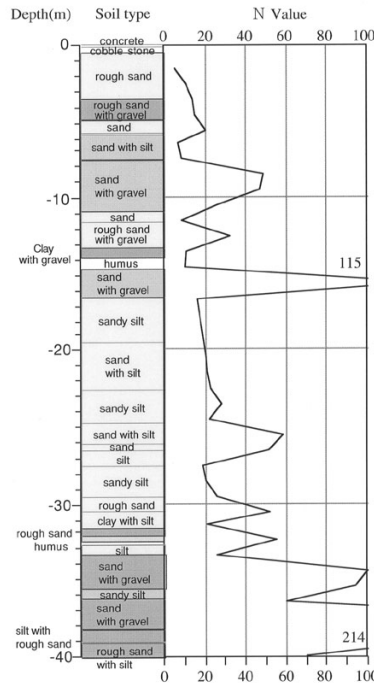


Figure 3: Soil profile at the NTT Kobe Ekimae building

### SEISMIC MOTIONS AT THE NTT KOBE EKIMAE BUILDING

The seismographs shown in Figure 2 are situated on the 8th floor and the 3rd basement of the NTT Kobe Ekimae Building. The sense of the seismographs was adjusted in the direction of the building axis, namely the direction of the building's length-wise side (N309°E), the building's shorter width-wise side (N219°E), and in the vertical direction. The acceleration time histories of the observed seismic motions at the 8th floor and the 3rd basement in the direction of the building's length-wise side is shown in Figure 4. Seismic waves at ground level (GL) and GL-65m are estimated using the Fourier spectrum ratio obtained by microtremor measurement, which was conducted after the 1995 Hyogo-ken Nanbu Earthquake. Figure 5 shows the estimated time history at GL-65m. The maximum acceleration value at GL-65m is 328 cm/sec<sup>2</sup>. Figure 6 shows the Fourier spectrum ratios of GL to 3rd basement, and of GL to GL-65m, respectively. The dotted lines show the observed amplitudes by microtremor and the solid lines show the model amplitudes in Figure 6. The observed Fourier spectrum ratio of GL to the 3rd basement was about 8 times in the short period range under 0.4 seconds. However, considering the nonlinearity of the ground at the time of the earthquake, the seismic wave is estimated using the model that has an amplification factor of 2.5 times in the short period range. (<http://www.ntt-f.co.jp/rd/frame-jks.html>)

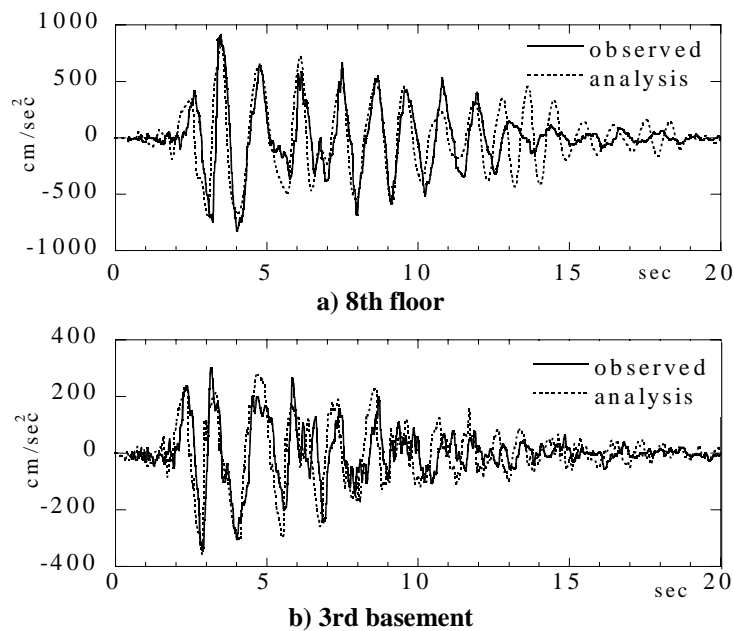
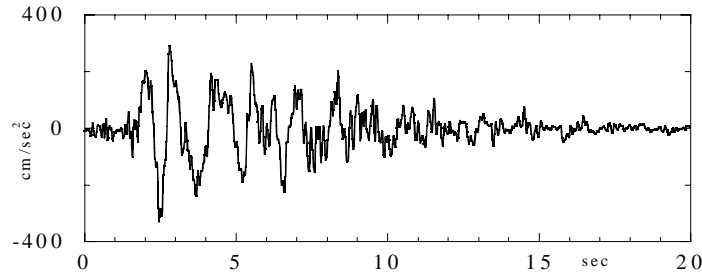
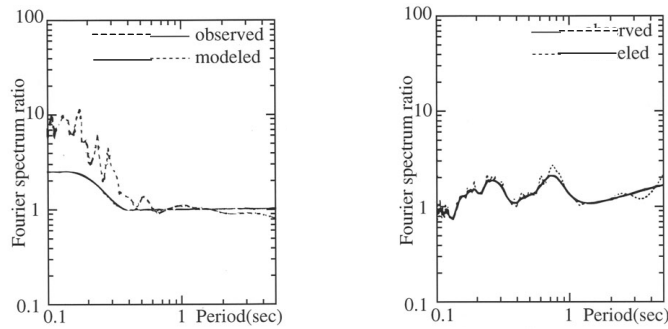


Figure 4: Comparison of acceleration time histories between observed seismic waves and analytical ones



**Figure 5: Acceleration time history of estimated seismic wave at ground level –65m (GL-65m)**



**a) GL to 3rd basement**

**b) GL to GL-65m**

**Figure 6: Fourier spectrum ratio by microtremor measurement**

### THE EXPRESSION OF THE DYNAMIC SOIL-STRUCTURE INTERACTION ANALYSIS MODEL

In this paper, a dynamic soil-structure interaction analysis was conducted in the direction of the building's length-wise side (N309°E) where a substantial input acceleration was observed. In order to perform the two-dimensional nonlinear analysis using step-by-step integration method, a finite element method model shown in Figure 7 was substituted for the soil structure from GL to GL-65m and the building. The base of the model was set as a stiff basement and the boundaries at the side of the model connected with the free field were set as a viscous boundary. The geological data of soil sediment shown in Table 1 was designated as the initial value. The strain-dependent characteristic referred the general soil sediment in Japan was expressed as a modified R-O model shown in Figure 8. The reference strain was set to be 0.05% when the shear modulus ratio was at 50%. The multi lumped mass models were substituted for the building on the ground. The beams of the building basement were modeled on rigid bodies and the weight and stiffness were distributed among the pillar positions for the building basement. The physical properties of building models are shown in Table 2.

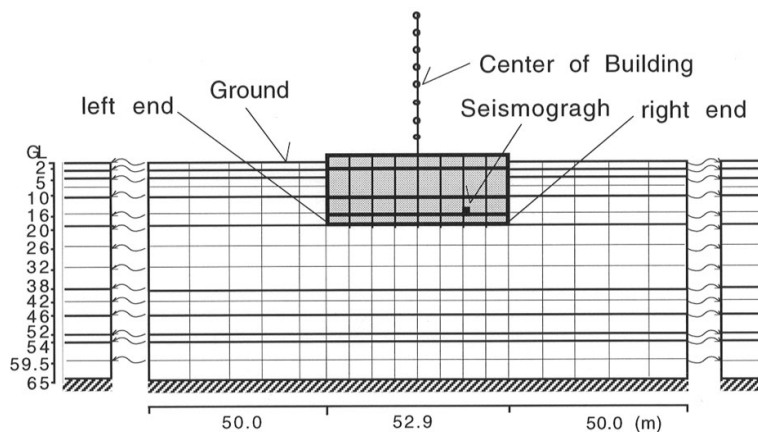


**Figure 7: Two-dimensional finite element method model (in m)**

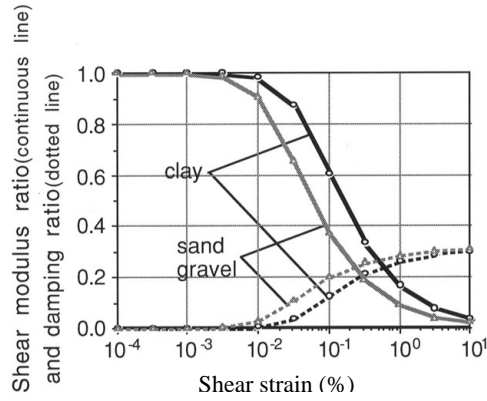


Figure 8: Variation in shear modulus and damping with shear strain (Modified R-O model)

Table 2: Physical properties of building models

Floor	Mass M(t)	Story height H(m)	Non-Linear				
			Stiffness(kN/cm)			Yield load(kN)	
			K1	K2	K3	Q1	Q2
9	2466	4.92	49460	11114	8260	8430	43000
8	3959	5.05	75150	16886	5185	20800	68460
7	4027	5.05	108500	24380	5642	31600	90300
6	4149	5.05	135070	30350	2566	40870	122520
5	4297	5.05	171190	38466	2739	48620	151600
4	4381	5.05	206400	46378	826	55000	169500
3	4495	5.05	266860	59963	4003	60080	178500
2	4633	4.40	488200	130301	123026	32020	204480
1	5068	4.40	1132250	302198	191350	33910	236530
-1	6853	6.50	912910	243656	98594	37710	252500
-2	7288	6.10	929780	248158	116223	41580	286000
-3	9712	3.58	—	—	—	—	—

Restoring force characteristics : Takeda model ( $f_A=0.4$ )

K1, K2, K3 : initial stiffness, second and third gradient, Q1, Q2 : first and second yield point

For the non-linear building model, the restoring force is set as a degrading tri-linear-type (Takeda model, stiffness reduction ratio: 0.4). The initial stiffness of the building (K1) is set by modifying the design model to match the primary natural period of 0.5 seconds that was deduced from the earthquake prior to the 1995 Hyogo-ken Nanbu earthquake. The yield load (Q1) and the second gradient (K2) are set by a parametric study based on the linear model of building. The damping factor to the initial stiffness is set at 3%. The primary natural period of the integrated soil-structure is 0.65 seconds.

The input seismic motion used for the analysis is the estimated seismic motion at GL-65m as described in Section 3, and is inserted vertically from the bottom of the two-dimensional FEM model.

### THE ESTIMATION OF THE SEISMIC RESPONSE

Figure 4 shows the comparison of acceleration time histories of the 8th floor and the 3rd basement between the observed seismic motions and the analytical ones. Their acceleration response spectra ( $h=5\%$ ) are shown in Figure 9. The analytical seismic motions are similar to the observed ones in the peak values and in the longer period range than 0.2 seconds.

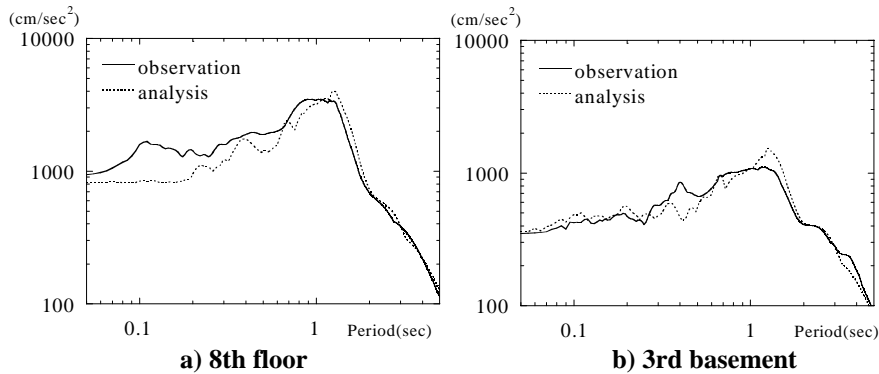
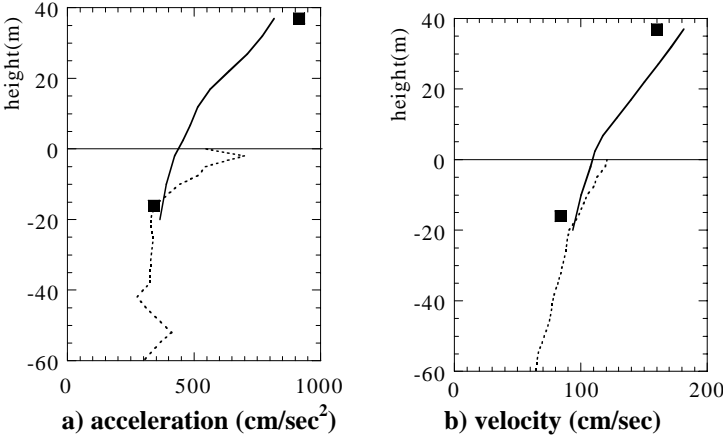


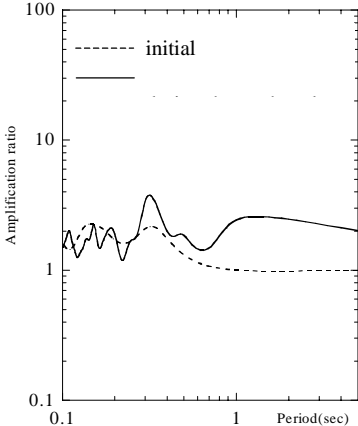
Figure 9: Comparison of acceleration response spectra between observed seismic waves and analytical ones

Figure 10 shows the distribution of the maximum response acceleration and velocity for the building and the free field. In comparison to the maximum response at the ground surface of the free field (548gal, 120kine), the maximum response at the 1st floor of the building shows approximately 17% less acceleration and approximately 7.5% less velocity. The input loss is caused by the soil-structure interaction effect.



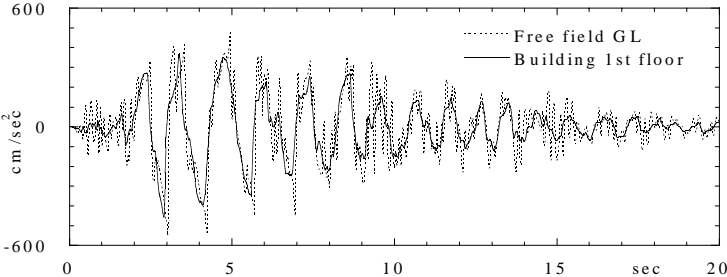
**Figure 10: Maximum acceleration and velocity distribution**

Figure 11 shows the comparison of amplification ratio between at initial condition and during the earthquake. The former is obtained by the one-dimensional linear ground model ( $\eta=5\%$ ) using the initial stiffness shown in Table 1. The latter is the Fourier spectrum ratio of GL to GL-65m in the free field on the nonlinear analysis. The large component is shown in the period of 0.8 seconds or more in the Fourier spectrum ratio, in spite of the fact that the site amplification ratio is not large in these period ranges. This feature indicates that the site nonlinearity, the soil nonlinearity occurring on the propagation of seismic wave in the surface soil, has a large influence on the amplification characteristics of the surface soil.

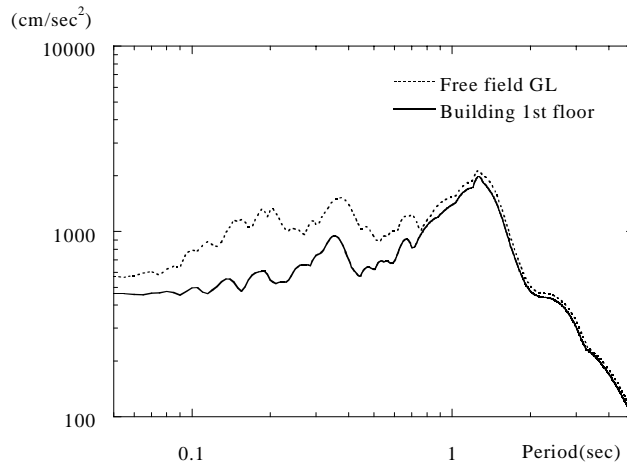


**Figure 11: Comparison of the amplification ratio between at the initial condition and during the earthquake**

Figure 12 shows the acceleration time histories at the ground surface of the free field and 1st floor of the building. Figure 13 shows the acceleration response spectrum ( $\eta=5\%$ ) of each. The amplitude at 1st floor of the building is smaller than at the ground surface of the free field, and the input loss is recognized in the period components of 0.8 seconds and less.

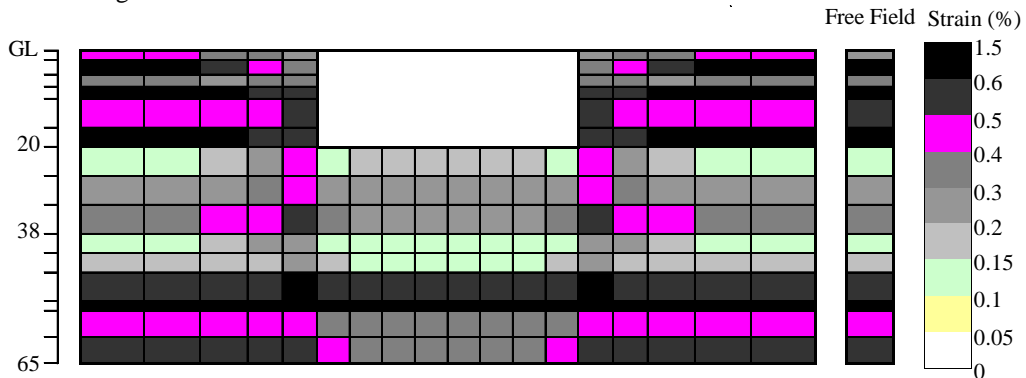


**Figure 12: Comparison of acceleration time histories between 1st floor of the building and ground surface of free field**



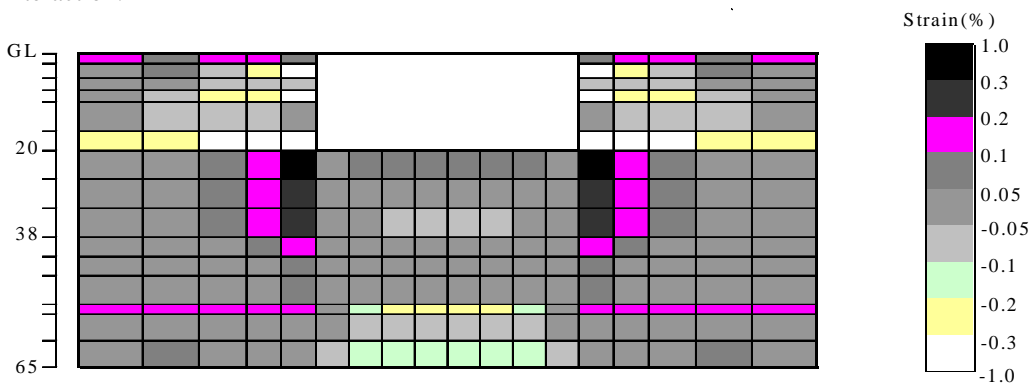
**Figure 13: Comparison of acceleration response spectra between 1st floor of the building and ground surface of free field**

Figure 14 shows the distribution of the maximum shear strain  $\gamma_{xy}$  with that of free field. The shear strain just under the building is small. On the other hand, large shear strains are shown diagonally downward to the outside of building. Especially in the sand layers from GL-32m to GL-38m near the building, large shear strains more than 0.43% are recognized.



**Figure 14: Distribution of maximum shear strain  $\gamma_{xy}$**

Figure 15 shows the distribution of the maximum shear strain related to the soil-structure interaction, which is obtained from subtracting the maximum shear strain of the free field from that of each element. Near the corners of building foundation, the maximum shear strain increases by 0.33% to 0.43% related to the effect of the soil-structure interaction.



**Figure 15: Distribution of maximum shear strain related to soil-building interaction**

Figure 16 shows the vertical displacement time histories at the left end and the right end of building foundation. Because the left end and right end of building foundation moved vertically in the converse phase, the rocking is approved. From these figures, it is found that the local 0.33% increase in the shear strain near the corner of

building foundation were caused by rocking of the building. The building rocked in a period of 1.2 seconds. The maximum displacement by the rocking at the 8th floor of building is 7.2cm, that is 18% of the total horizontal displacement. The local nonlinearity, the soil nonlinearity caused by the stress concentration near the face of building foundation to the soil, has large effect on the seismic response characteristics of the building.

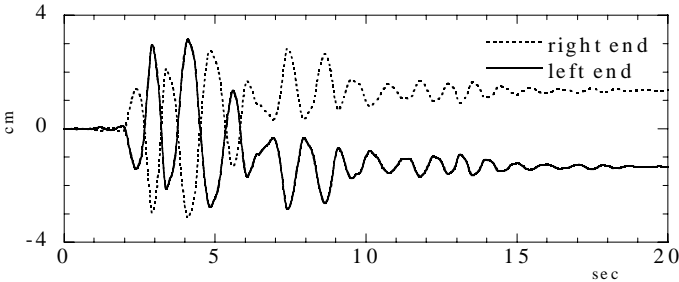


**Figure 16: Vertical displacement time histories at end of building foundation**

Figure 17 shows the relationship between the story shear force and the relative story displacement of each floor. The story deformation angle is approx. 1/180 from the 2nd to the 5th story. Considering the 8-story SRC structure, this result corresponds well to the extent of the actual damage to the building.

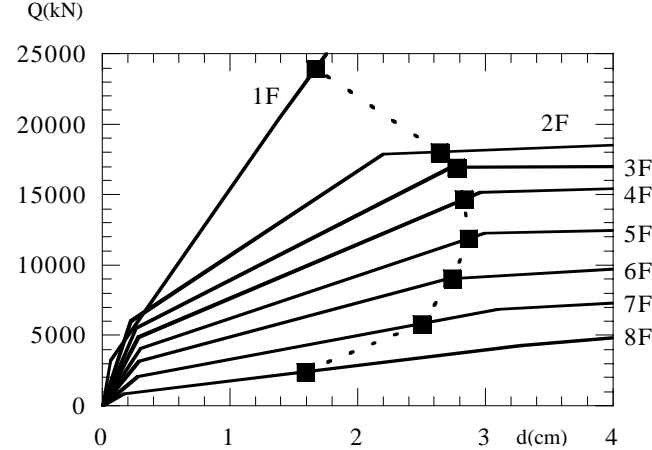


**Figure 17: Relationship between story shear force and relative story displacement**

**CONCLUSIONS**

The seismic response characteristics of the NTT Kobe Ekimae Building during the 1995 Hyogo-ken Nanbu Earthquake were estimated by means of a nonlinear dynamic soil-structure interaction analysis using the two-dimensional FEM model. The following findings were noted:

- 1) The nonlinear soil-structure interaction analysis model described in this paper was able to simulate the observed seismic waves of the building and represent the damage to the building accurately.
- 2) The input loss of the ground motion from the free field to the building became apparent at the period component of 0.8 second and less, with a loss of approx. 17% in acceleration and approx. 7.5% in velocity.
- 3) The site nonlinearity has a large influence on the amplification characteristics of the surface soil, and the local nonlinearity caused by rocking of building has a large influence on the seismic response characteristics of the building.

**REFERENCE**

Dohi H., Inaba T., Sato T., Ninomiya T., Okuta K., and Akagi H. (1998) "Seismic response analysis of the NTT Kobe Ekimae building during the Hyogo-ken Nanbu Earthquake of 17<sup>th</sup> January, 1995" *Proc. 10JEES(Japanese)*, pp1803-1808.